Trop J Nat Prod Res, January 2025; 9(1): 362 - 368 ISSN 2616-0684 (Print)
ISSN 2616-0692 (Electronic)

Tropical Journal of Natural Product Research

Available online at https://www.tjnpr.org

Original Research Article

Comprehensive Exploration of Ferulic Acid from Corn Leaves: Extraction, Structural Characterisation, HPLC Quantification, and Anti-inflammatory Evaluation through *In Silico* Docking, Molecular Dynamics Simulation, and *In Vitro* Studies

Rajeshwari S[1], Surendra K Chowdary[2], Dileep A[2], Suresh Joghee*[1], Erica Alves[2], Bannimanth Gurupadayya*[2], Nithin Mohan[3], Prashantha B. Kumar[2], Subba V. Madhunapantula[3]

[1]*Department of Pharmacognosy, JSS College of Pharmacy, JSS AHER, Mysore, Karnataka, India*
[2]*Department of Pharmaceutical Chemistry, JSS College of Pharmacy, JSS AHER, Mysore, Karnataka, India*
[3]*Center of Excellence in Molecular Biology and Regenerative Medicine, Department of Biochemistry, JSS Medical College, JSS AHER, Mysore, Karnataka.*

ARTICLE INFO

Article history:
Received 01 November 2024
Revised 13 November 2024
Accepted 21 December 2024
Published online 01 February 2025

ABSTRACT

Ferulic acid, a phenolic compound with notable anti-inflammatory and antioxidant properties, has drawn significant interest for its therapeutic potential. Maize leaves, an abundant agricultural byproduct, are a sustainable source of ferulic acid, though efficient extraction and characterisation methods remain underdeveloped. This study presents an optimised protocol for isolating and characterising ferulic acid from maize leaves while evaluating its anti-inflammatory potential. The extraction process utilised aqueous methanol treatment to remove secondary metabolites, followed by alkali hydrolysis for ferulic acid isolation. The compound was purified via column chromatography, with temperature optimisation enhancing yield. Structural characterization was conducted using TLC, FT-IR, ^{1}H, and ^{13}C NMR. Quantitative analysis was achieved using a validated HPLC method. *In silico* docking studies demonstrated strong binding interactions between ferulic acid and p38 MAPK, a key inflammation-related protein, with docking scores comparable to those of bosutinib, a known anti-inflammatory agent. Additionally, *in vitro*, bovine serum albumin (BSA) denaturation assays revealed a dose-dependent inhibition of BSA denaturation, with significant effects observed at 100 µM. This study establishes an efficient method for extracting and characterising ferulic acid from maize leaves and highlights its promising anti-inflammatory properties, suggesting its potential for therapeutic applications.

Keywords: Ferulic acid, Maize leaves, Anti-inflammatory, Antioxidant, *In silico* docking, p38 MAPK protein

Introduction

Secondary metabolites, previously regarded as incidental byproducts of plant metabolism, are now recognised as pivotal bioactive compounds with substantial pharmacological potential. These naturally occurring secondary metabolites have been leveraged in modern pharmaceuticals due to their wide-ranging applications and therapeutic relevance.[1] Maise, a crop with high yield and productivity. It is India's third most significant crop, following rice and wheat.[2] It is predominantly cultivated as a summer crop, accounting for 80% of cropland, with an estimated production of 15.5 million tons in 2015–16.[3] Maize (*Zea mays*), a cornerstone of global food security and agricultural economies, is essential for food and feed and represents an underexplored source of valuable phytochemicals.[4] Among its agricultural byproducts, maize leaves remain underutilised despite their robust structure and fibrous composition.

*Corresponding author. E mail: jsuresh@jssuni.edu.in

Tel: +919480197611

Citation: Rajeshwari S, Chowdary SK, Dileep A, Joghee S, Alves E, Gurupadayya B, Nithin Mohan, BR Kumar P, Madhunapantula SV. Comprehensive Exploration of Ferulic Acid from Corn Leaves: Extraction, Structural Characterisation, HPLC Quantification, and Anti-inflammatory Evaluation through *In Silico* Docking, Molecular Dynamics Simulation, and *In Vitro* Studies. Trop J Nat Prod Res. 2025; 9(1): 362 – 368
https://doi.org/10.26538/tjnpr/v9i1.46

Official Journal of Natural Product Research Group, Faculty of Pharmacy, University of Benin, Benin City, Nigeria

One noteworthy phytochemical in maize leaves is ferulic acid (4-hydroxy-3-methoxycinnamic acid), a phenolic compound derived from caffeic acid.
This compound is primarily linked to plant cell wall polysaccharides, contributing to lignin formation and structural rigidity (Figure 1).[5]

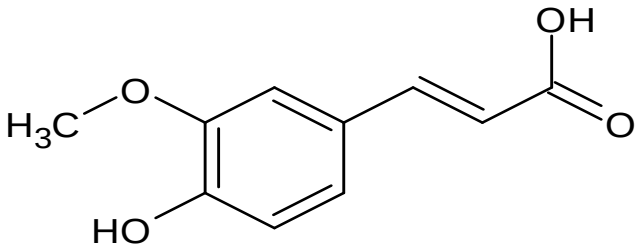

Figure 1: Structure of ferulic acid

Ferulic acid is widely distributed in vegetables, fruits, beverages (e.g., coffee, beer), and traditional Chinese medicinal herbs. Its antioxidant properties have been recognized globally, and it has been used as a dietary ingredient for preventing lipid peroxidation.[6]
Ferulic acid demonstrates therapeutic potential across various diseases, including neurological disorders, diabetes, cardiovascular conditions, inflammation, and bacterial/viral infections.[7] Commercialisation of ferulic acid extracts offers environmental and economic benefits, extending its utility in pharmaceuticals, functional foods, and nutraceuticals. Various methods for its extraction—alkaline, acidic, and enzymatic—are well-documented in the literature.[8] Functionally, ferulic acid improves insulin sensitivity, modulates lipid profiles, lowers blood pressure, and enhances vascular function.[9] Its

cardioprotective effects are mediated through the regulation of signalling pathways such as NF-κB and Nrf2/HO-1, which mitigate oxidative damage and inflammation.[10] Ferulic acid has extensive applications in the food, pharmaceutical, and cosmetic industries, attributable to its low toxicity, high bioavailability, antioxidant, and antibacterial properties.[2] Recent studies highlight its anti-inflammatory effects, such as mitigating LPS-induced inflammation in bovine endometrial epithelial cells by inhibiting NF-κB and MAPK pathways.[11] Moreover, ferulic acid reduces testicular inflammation in rats by modulating pro-inflammatory and anti-inflammatory markers through the JAK-STAT pathway.[12] Its efficacy in alleviating LPS-induced kidney damage has also been reported, with minimal adverse effects, through activation of Nrf2/HO-1 proteins and suppressing NF-κB signaling.[13]

This study addresses the underutilisation of maize leaves by developing an innovative extraction and characterisation method for ferulic acid. The novelty of this research lies in bridging the existing knowledge gap by focusing on maize leaves as a novel source of ferulic acid and integrating advanced extraction techniques with robust analytical methods, including Thin-Layer Chromatography (TLC), Fourier Transform Infrared Spectroscopy (FT-IR), and Nuclear Magnetic Resonance (NMR) spectroscopy for precise identification and quantification. Furthermore, the study explores the anti-inflammatory properties of ferulic acid through *in-silico* docking and *in vitro* assays, linking its biochemical attributes to therapeutic potential. Byoptimising the extraction process and validating the bioactivity of ferulic acid, this research enhances the value of maise leaves, contributing to sustainable agricultural practices and the development of natural anti-inflammatory agents, thus addressing the aforementioned knowledge gaps and demonstrating the relevance of its methodologies in achieving these objectives.

Materials and Methods

Chemicals and reagents

Commercial-grade chloroform, hexane, methanol, ethyl acetate, silica gel, and cotton were obtained from SRL, India. HPLC-grade orthophosphoric acid, acetonitrile, and Millipore water were sourced from Merck, India. LC-MS grade methanol and NMR-grade deuterated methanol were also procured from Merck, India. Analytical TLC plates precoated with silica gel 60 F_254, and silica gel (60–120 mesh) were acquired from Merck (Mumbai, India). Aspirin and bovine serum were purchased from Sigma-Aldrich.

Collection of Plant Materials

Corn leaves were collected in October 2023 from agricultural fields in Channapatna (Latitude: 12.6530°N, Longitude: 77.2050°E), India, near Mysore in the southern region of Karnataka. The plant material was identified and authenticated by Dr. Suresh Joghee, a botanist from our institute, and a voucher specimen was deposited in the institutional repository for future reference. The collected leaves were naturally dried under sunlight, reducing their initial weight from 5 kg to 100 g post-drying.

Extraction of Ferulic Acid

Ferulic acid extraction was performed following the procedure outlined by Aarabi *et al.* [14] Corn leaves were sourced from various agricultural fields in the Mysuru region, dried under sunlight, and ground into powder. The powdered material was extracted with 50% aqueous methanol for 48 hours, followed by filtration. The filtrate was concentrated to yield 10 g of a semisolid brown paste (10% w/w yield). Residual plant material was subjected to alkaline extraction using a sodium hydroxide solution (pH 12) in a 10:1 ratio of sodium hydroxide to the plant material. The mixture was stirred on a hot plate at 70ºC for 2 hours. The ethyl acetate extraction was followed by evaporation using a rotary evaporator at 45ºC and 25 mbar, thus yielding a brown residue.

Isolation and Characterisation of Ferulic Acid

The crude ethyl acetate fraction was subjected to column chromatography on silica (50 g; 100–200 mesh) using chloroform (1 L) as the eluent.[15] The column was eluted with 100% chloroform, and fractions were collected (Fr A–Fr I) with 30 mL per fraction. Thin-layer chromatography (TLC) was used to monitor the fractions, and impurities were discarded.[16] Fractions J, K, L, M, and N were combined and stored overnight. Crystals from these fractions were examined and further analysed by ^{1}H and ^{13}C NMR spectroscopy.

HPLC method development and validation

Chemicals and Reagents

All chemicals and reagents utilised in the HPLC method development and validation were of high-purity grade to ensure accuracy in analysis. The primary reagents included ortho-phosphoric acid (Merck), acetonitrile (SDFCL), and Milli-Q purified water, which provided the essential solvents and mobile phases for the HPLC system. Each reagent was selected for compatibility with high-performance liquid chromatography to prevent contamination and ensure method sensitivity.

Analytes

The target analyte in this study was ferulic acid, a compound known for its bioactive properties. A high-purity standard of ferulic acid (assay purity 99%) was obtained from Thermo Fisher Scientific, with batch number 156360250, to ensure consistent quality during method validation.

Instrumentation

The HPLC method was developed and validated using a Shimadzu UFLC system paired with LabSolutions software for data acquisition, which provided precision and reproducibility in chromatographic analysis (Table 1).[17] Additional instruments utilized included an analytical balance (Shimadzu AY220) for accurate sample and standard preparation, a Genius 3 IKA® Vortex for mixing, and a REMI RM-12CDX centrifuge for sample clarification. Each instrument was chosen to meet the precision and accuracy requirements for successful method validation.

Table 1: Final HPLC optimised chromatographic conditions to separate ferulic acid

S.no	Parameters	Conditions
1.	Instrument Model	Shimadzu LC-2010A HT
2.	Column	Shim pack C-18 Column (150×4.6mm, 5µm)
3.	Mobile phase	Acetonitrile (A) and 0.1% orthophosphoric acid (B) in water at a ratio of 90:10 v/v
4.	Run time	10 minutes
5.	Rate of flow	1.7 mL min^{-1}
6.	Injection volume	10 µL
7.	Column oven temperature	40˚C
8.	Detector	Photodiode array detector
9.	Detection wavelength	320 nm

Preparation of solutions

Standard stock solution:

The ferulic acid standard (25 mg) was measured accurately and transferred into a 25 mL volumetric flask. After adding 10 mL of acetonitrile, the solution was sonicated for 5 minutes. The volume was then adjusted with acetonitrile to obtain a final 1000 µg/mL concentration.

0.1% orthophosphoric acid

Added 1 mL of phosphoric acid to 999 mL of HPLC water to obtain 0.1% orthophosphoric acid.

Sample solution preparation
A 1000 µg/mL solution was prepared by dissolving 10 mg of ferulic acid crystals in 10 mL of acetonitrile. From this stock solution, 1 mL was transferred into a 10 mL volumetric flask and diluted with the appropriate diluent to achieve a final 100 µg/mL concentration.

Analytical method validation
Using ICH recommendations (Q2-R2), the established HPLC technique for ferulic acid estimation was validated. The comprehensive methodology and results of the HPLC validation, including system suitability, accuracy, precision, linearity, robustness, and forced degradation studies, are detailed in the supplementary file.

Molecular docking studies
Macrophages play a vital role in regulating inflammation during the innate immune response. Mitogen-activated protein kinases (MAPKs), serine, and threonine kinases control cellular responses in normal and disease states.[18] p38 MAPKs are vital for the production of key inflammatory mediators. They are involved in generating TNF-α, which plays a significant role in inflammatory responses, and COX-2, an enzyme essential for prostaglandin synthesis. The signalling pathways of p38 MAPKs are fundamental in regulating these inflammatory processes.[19,20]

In the computational analysis, molecular docking and dynamics simulations were carried out using Schrödinger Suite 2023-3, with Maestro 13.7 employed for the simulations, as described by Alves *et al*. (2024) in their study on targeting breast cancer through FN3K enzyme inhibitors.[21] The Glide module of this software was employed to conduct a comprehensive search of the ligand's conformational, orientational, and positional space within the binding pocket. Molecular dynamics simulations were executed with the Desmond module over a 100 ns time frame, applying the default relaxation settings. The simulations were conducted under normal pressure and temperature (NPT) conditions at 300 K and 1.013 bars. Desmond facilitated the generation of various thermodynamic variables and high-quality long-time-scale simulation trajectories. The data were analysed using Radius of Gyration (Rg), Root-Mean-Square Deviation (RMSD), and Root-Mean-Square Fluctuation (RMSF) metrics to evaluate the dynamics of the molecular simulations.

Docking Protocol
Protein Preparation
For the current study, the p38 mitogen-activated protein kinase (MAPK) structure (PDB ID: 3GP0) was utilised, available at https://www.rcsb.org/structure/3GP0. Protein preparation was performed with the Protein Preparation Wizard in the Schrödinger Suite, including bond order assignment, hydrogen addition, and water removal. The structure was then refined using constrained molecular mechanics with the OPLS_2005 force field until the RMSD of heavy atoms reached 0.3 Å. This refinement also involved assigning tautomers and protonation states.

Ligand Preparation
The 3D structure of ferulic acid was retrieved from the PubChem database (https://pubchem.ncbi.nlm.nih.gov/) and converted to PDB format using Discovery Studio Visualizer. Its energy was minimised with the MMFF97 force field before converting it to pdbqt format for docking studies.

In-vitro BSA denaturation method
The anti-inflammatory properties of ferulic acid were evaluated using an *in vitro* BSA denaturation assay, following the principles outlined by Ameena *et al*. in their studies (2017) [22,23] Different concentrations of ferulic acid (1, 10, and 100 µM) and Aspirin (1, 10, and 100 µM) were incubated with 1 mg/mL BSA at 70°C for 10 minutes. Absorbance was measured at 660 nm using a UV-visible spectrophotometer, including readings from a positive and negative control (1 mg/mL BSA heated at 70°C for 10 minutes). The percentage inhibition of denaturation was calculated using the equation 1.

$$\%\ Inhibition\ of\ denaturation = \left(1 - \frac{T}{C}\right) x\ 100 \qquad \textbf{Equation (1)}$$

T represents the absorbance of the test sample, and C denotes the absorbance of the negative control (excluding the test sample or reference drug).

Results and discussion

After the initial aqueous methanol extraction, the extraction process yielded 10 g (10% w/w) of a semisolid brown paste. This step facilitated the separation of the soluble fractions, primarily containing ferulic acid and other polar compounds. The subsequent alkaline extraction using sodium hydroxide (pH 12) followed by ethyl acetate partitioning resulted in the isolation of a brown residue weighing **2 g (2% w/w)**. This additional step ensured the recovery of ferulic acid bound to the plant matrix, which is typically released under alkaline conditions. The overall yield reflects the efficiency of the two-step extraction process, with alkaline hydrolysis playing a critical role in liberating bound ferulic acid. These results are consistent with previous studies employing similar extraction protocols, where comparable yields of ferulic acid were reported, emphasizing the method's robustness. The isolated Ferulic acid was identified using different spectrophotometric methods. Firstly, to identify ferulic acid in corn leaf extract, the thin-layer chromatography (TLC) solvent system was optimized by varying the ratios of nonpolar to polar solvents. The final mobile phase was optimized to 9.7 mL chloroform, 0.3 mL methanol, 1 drop of formic acid (FA), and 1 drop of water. As depicted in Figure 2, the Rf value of the sample closely matched that of the standard, confirming that the isolated compound from corn leaves was ferulic acid. Also, the identity of the obtained ferulic acid crystals was confirmed through mass spectrometry (Figure 3). The observed molecular weight of 193.0 g/mol in negative ESI mode closely corresponds to the theoretical molecular weight of 194.18 g/mol for ferulic acid. The high congruence between the theoretical and experimental values supports the identification of ferulic acid. Mass spectra were acquired on a WATERS ACQUITY Rda with a fragmenter voltage of -160 V and a collision energy of -17 eV.
Furthermore, the FT-IR spectrum of crystallized ferulic acid was recorded using a Shimadzu FTIR-8400S spectrometer (Figure 4). Sample pellets were prepared using a KBr press model M-15 from Techno Search Manufacturers. The FT-IR spectrum confirmed the key functional groups characteristic of ferulic acid. The broad, strong band at 3,331.08 cm^{-1} corresponds to the OH group of the phenolic compound. The C-H stretching of the aromatic ring is observed at 2,925.82 cm^{-1}, while a band represents the carbonyl group (C=O) at 1,649.02 cm^{-1}. The stretching vibration of the methyl group (C-H) appears at 1,328.87 cm^{-1}, and the C=C vibration of the aromatic ring was detected at 692.77 cm^{-1}.

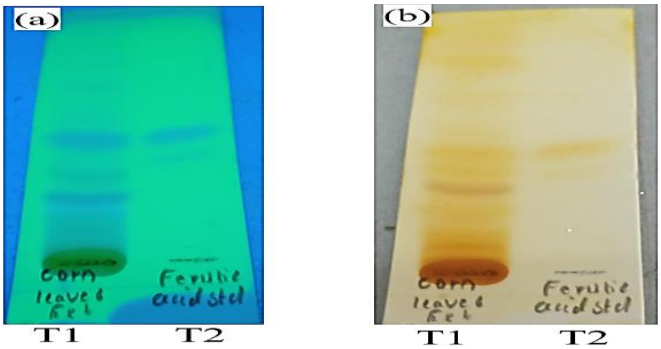

Figure 2: Identification of ferulic acid by TLC (a)TLC under UV (254 nm) (b) TLC treated with iodine vapours.

ISSN 2616-0684 (Print)
ISSN 2616-0692 (Electronic)

Similarly, the ^{1}H NMR spectrum of ferulic acid, recorded with a Varian 300 MHz NMR and CD_3OD as a solvent, showed two doublets at δH 6.27 (1H, d, J = 15.90 Hz) and 7.55 ppm (1H, d, J = 15.89 Hz), three aromatic signals at 7.15 ppm (1H, dd, J = 8.48 and 2.19 Hz), 7.02 ppm (1H, d, J = 8.47 Hz), and 7.61 ppm (1H, d, J = 2.17 Hz), and methoxy protons at 3.87 ppm (3H, s) (Figure 5). The ^{13}C NMR spectrum indicated the presence of ferulic acid with a carboxylic acid carbonyl signal at δC 169.59 ppm (C-9), olefinic carbons at 115.01 and 145.52 ppm, aromatic carbons at 114.43, 122.58, and 126.33 ppm, oxygenated aromatic carbons at 147.90 and 149.02 ppm, and a methoxy carbon at 54.97 ppm (Figure 6).

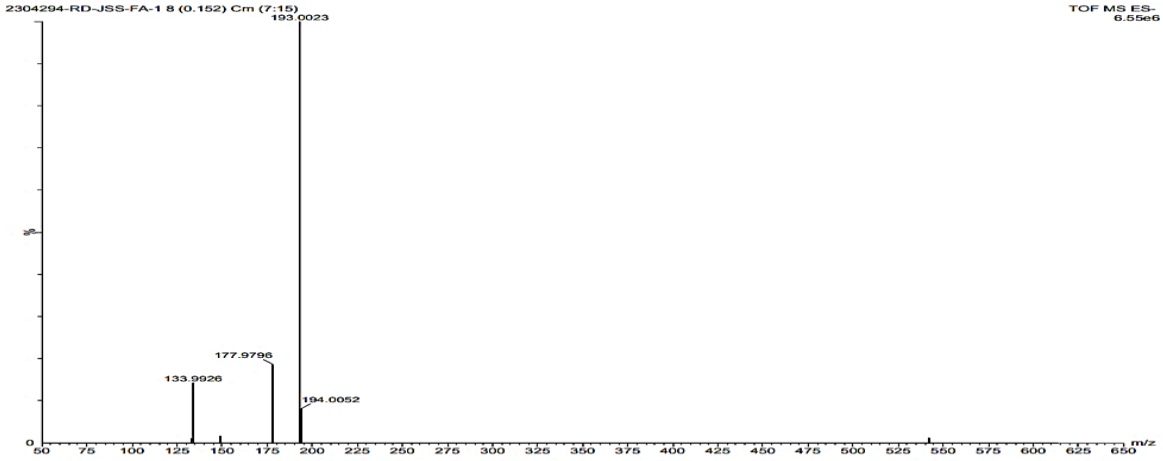

Figure 3: Mass chromatogram of Ferulic acid at (- ve) ESI mode.

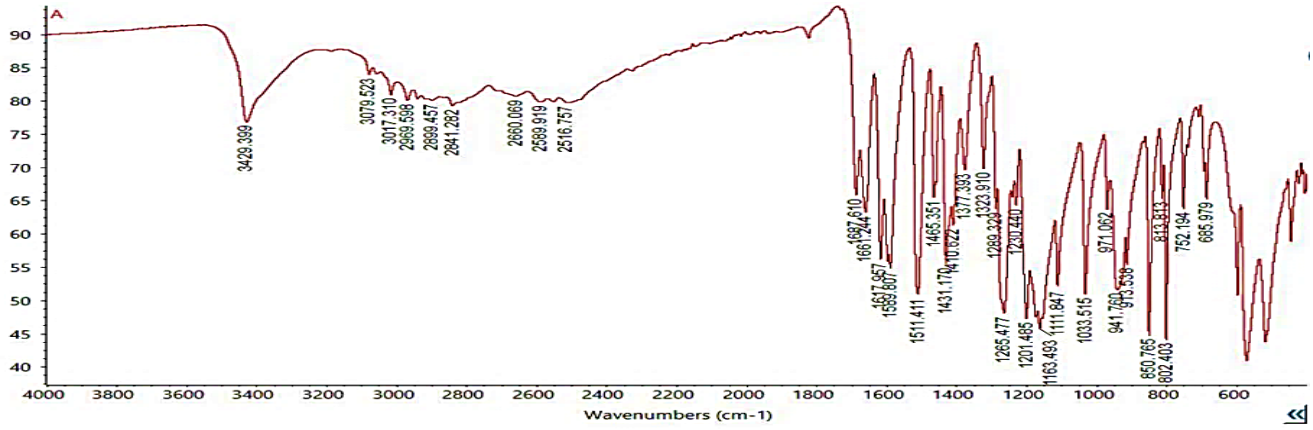

Figure 4: FTIR spectrum of isolated ferulic acid crystals from the extract of *Corn leaves*.

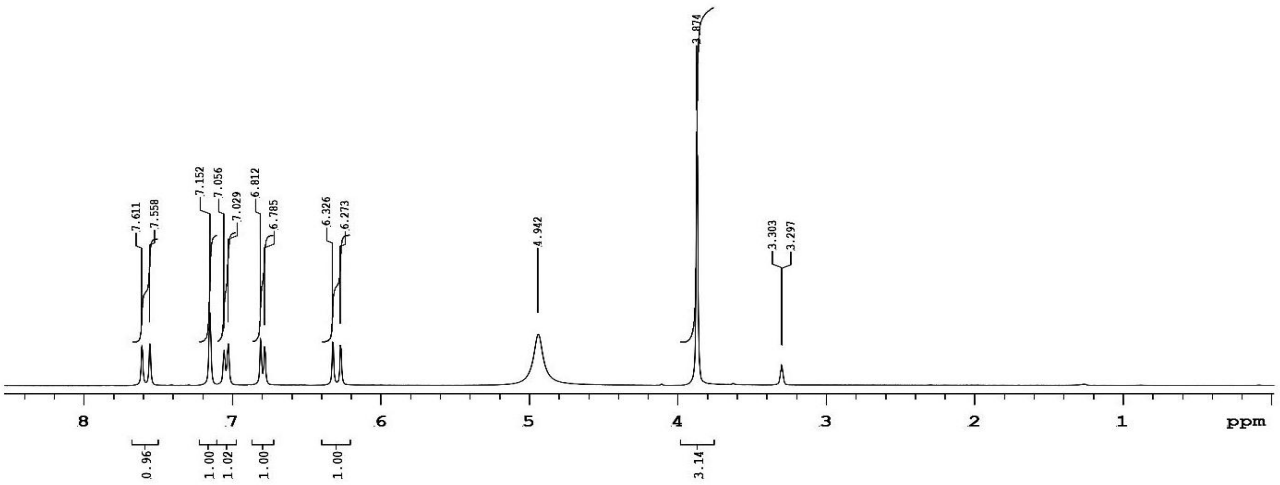

Figure 5: ^{1}H-NMR spectrum of isolated ferulic acid from *Corn leaves*

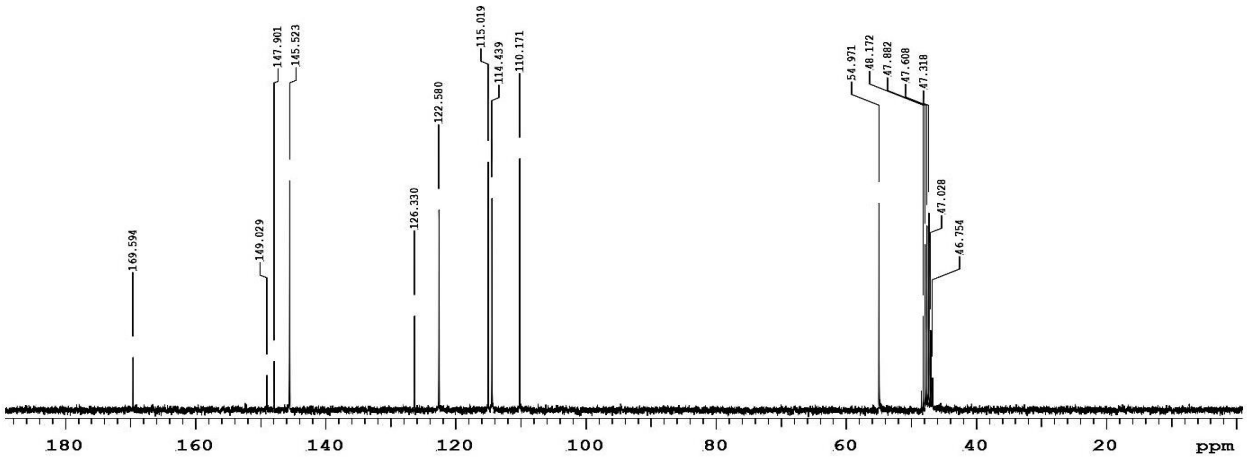

Figure 6: ^{13}C NMR spectrum of isolated ferulic acid from *corn leaves.*

The HPLC method for the isolation and detection of ferulic acid used a mobile phase consisting of acetonitrile (A) and 0.1% ortho-phosphoric acid in water (B) in a 90:10 v/v ratio. This phase composition resulted in a pronounced peak for standard ferulic acid at a retention time (RT) of 3.4 minutes (Figure 7). The chromatographic profile exhibited a significant tailing effect, indicating a symmetrical and well-resolved peak. The theoretical plate count was determined to be 4014.4. These findings underscore the efficacy of the ortho-phosphoric acid and acetonitrile in a water mixture for achieving optimal chromatographic performance in the isolation of ferulic acid, as presented in Table 1. The presence of ferulic acid in the sample is corroborated by the chromatogram (Figure 8), which shows a peak at a retention time of 3.4 minutes.

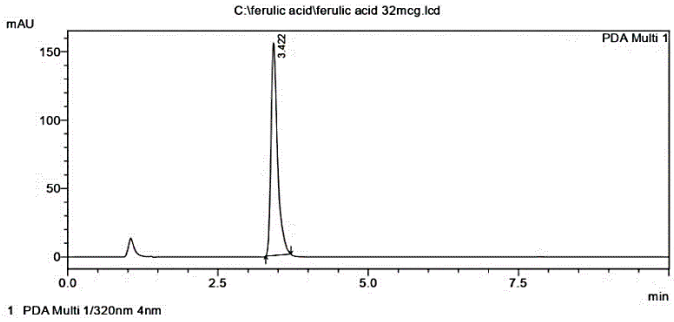

Figure 7: HPLC chromatogram of standard ferulic acid

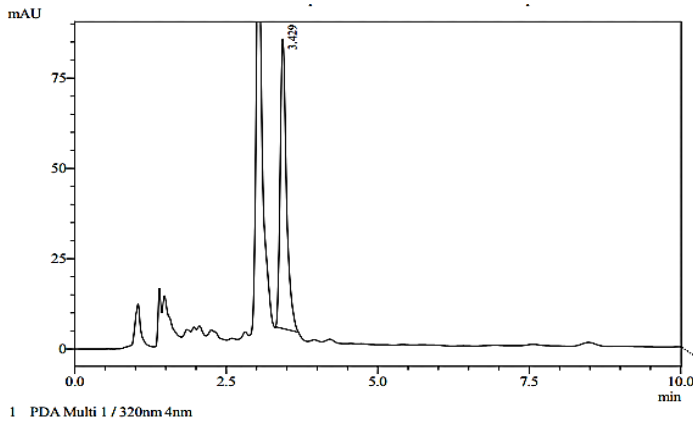

Figure 8: HPLC chromatogram of isolated ferulic acid from *corn leaves*

Ferulic acid concentration (x) was determined from the calibration curve using the regression equation 2:

$$y = 36833x - 16309 \qquad Equation\ (2)$$

Where y (Peak area response of Ferulic acid in extract sample) = 579992. From equation 2, Ferulic acid concentration (x) was computed as 16.18 µg/mL. The molecular docking study focused on the binding interactions of ferulic acid and the control drug bosutinib with p38 mitogen-activated protein kinases (MAPKs), which play a pivotal role in inflammatory processes. The binding site was identified through a structural analysis using the PDB file, which allowed for precise positioning of the ligands in the active site. The binding affinity was evaluated through docking scores, with ferulic acid and bosutinib showing scores of -5.548 and -5.408, respectively. These scores indicate that ferulic acid binds more effectively than bosutinib, suggesting it may be a more potent inhibitor of p38 MAPK. The lower docking score of ferulic acid suggests a stable interaction within the protein's active site, where it engages several critical residues, including ARG149, ARG70, HIS148, and ILE146. These residues are vital for the catalytic activity of p38 MAPK, and their interactions with ferulic acid imply that it may disrupt the enzyme's functionality, thereby potentially reducing inflammatory responses. Figure 9(a) illustrates the interactions of the control drug bosutinib with p38 MAPK, while Figure 9(b) presents the 2D depiction of ferulic acid's bonding with these residues.

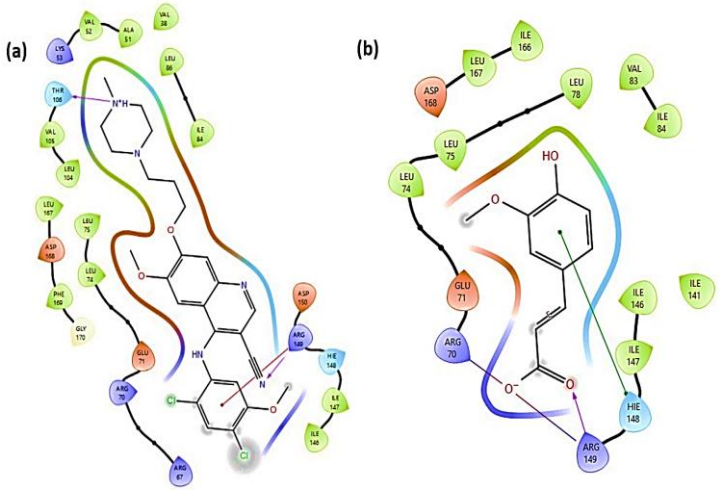

Figure 9 (a): 2D interaction diagram of standard bosutinib with p38 MAPK. (b) 2D interactions of ferulic acid with the p38 MAPK

Molecular dynamics (MD) simulations were employed to assess further the stability of the ferulic acid–p38 MAPK complex over time. Figure 10 displays the complex's root mean square deviation (RMSD) trajectory, which remained stable throughout the simulation. The RMSD fluctuation stayed within a narrow range, indicating that the binding conformation of ferulic acid in the active site is energetically favourable, further reinforcing its potential as an anti-inflammatory therapeutic.

The anti-inflammatory activity of ferulic acid was also assessed *in vitro* using the bovine serum albumin (BSA) denaturation method. Table 12 and Figure 11 present the dose-dependent inhibition of BSA denaturation achieved by ferulic acid at 1, 10, and 100 µM concentrations. Ferulic acid inhibited BSA denaturation by 0.7%, 1.9%, and 4.5% at these respective concentrations. In contrast, aspirin, a known anti-inflammatory agent, showed significantly higher inhibition rates of 4.4%, 6.5%, and 15.2% at the same concentrations, underscoring aspirin's more potent activity in this assay. The results in Figure 11 illustrate the standard error markers for both the standard and sample, clearly showing data variability. The findings indicate that ferulic acid exhibits significant inhibition of BSA denaturation in a dose-dependent manner; however, its efficacy is lower than that of aspirin at equivalent concentrations. This observation suggests that ferulic acid possesses anti-inflammatory properties but is less potent than aspirin under the conditions tested.

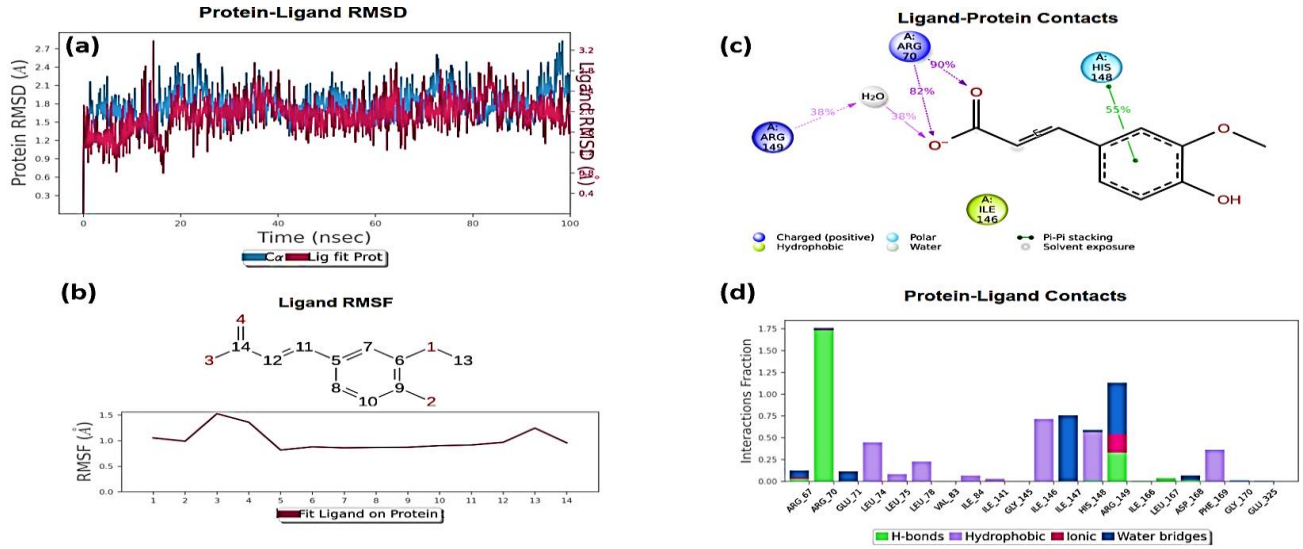

Figure 10: Typical MD simulation work for ferulic acid. (a) Protein RMSD is shown by the left y-axis, while ligand RMSD fit on protein is represented by the right y-axis. (b) The ligand RMSF graph. (c) A summary of the important interactions between proteins and ligands present for more than 30.0% of the simulation time. (d) The bar graph represents the various protein-ligand interactions in terms of hydrogen bonds, water bridges, hydrophobic and ionic interactions.

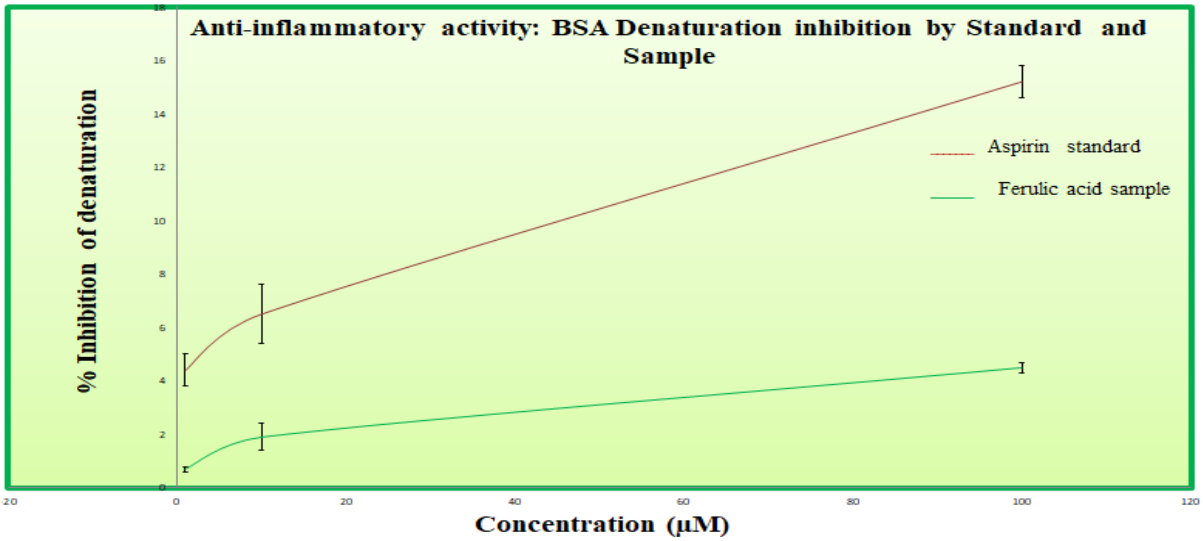

Figure 11: Bar graph illustrating the percentage inhibition of BSA denaturation by Aspirin (Standard) and Ferulic Acid (Sample), with standard error intervals

Conclusion

This study successfully identified and characterised ferulic acid from corn leaves using advanced analytical techniques, including TLC, FT-IR, NMR, and mass spectrometry, confirming its identity and purity. An optimized HPLC method demonstrated high selectivity, sensitivity, and reliability for quantification, with robust validation and degradation studies highlighting its stability under alkaline conditions but susceptibility to oxidative degradation. Molecular docking and MD simulations revealed strong binding of ferulic acid to p38 MAPK, suggesting potential inhibitory effects on inflammatory pathways. *In vitro*, assays supported its dose-dependent anti-inflammatory activity, though it was less potent than aspirin. Future studies will focus on expanding its bioactivity profile, optimizing its stability for pharmaceutical formulations, and investigating its synergistic effects

with other anti-inflammatory agents. Clinical trials will be critical for assessing its *in vivo* efficacy and safety while exploring its potential in treating chronic conditions such as cardiovascular diseases, diabetes, and neurodegenerative disorders.

Conflict of Interest

The authors declare no conflict of interest.

Authors' Declaration

The authors hereby declare that the work presented in this article is original and that any liability for claims relating to the content of this article will be borne by them.

Acknowledgments

The authors wish to acknowledge the Principal, JSS College of Pharmacy, Mysore, and JSS Academy of Higher Education and Research, Mysore, for providing the resources and facilities to complete the research.

References

1. Beladjal H, Bouhadi D, Belkhodja H. HPLC-DAD analysis and antioxidant potential of *Ferula assafoetida* resin ethanol extract. Trop J Nat Prod Res. 2024;8(4):6906-6910. Available from: https://doi.org/10.26538/tjnpr/v8i4.22
2. Hussain M, Qamar A, Saeed F, Rasheed R, Niaz B, Afzaal M, Ahmed A, Ahmad A, Anjum F. Biochemical properties of maize bran with special reference to different phenolic acids. Int J Food Prop. 2021;24(1):1468–1478. https://doi.org/10.1080/10942912.2021.1973026
3. Singh G, Jose S, Kaur D, Soun B. Extraction and characterisation of corn leaf fiber. J Nat Fibers.2020;19(5):1581–1591. https://doi.org/10.1080/15440478.2020.1787914
4. Matin M, Uddin S, Rohman M, Maniruzzaman M, Azad A, Banik B. Genetic variability and path analysis studies in hybrid Maize (*Zea mays* L.). Am J Plant Sci. 2017;8:3101–109. https://doi.org/10.4236/ajps.2017.812209
5. Zhang Z, Yang P, Zhao J. Ferulic acid mediates prebiotic responses of cereal-derived arabinoxylans on host health. Anim Nutr. 2021;9:31–38. https://doi.org/10.1016/j.aninu.2021.08.004.
6. Raj N, Siingh D. A critical appraisal on ferulic acid: the biological profile, biopharmaceutical challenges, and nanoformulations. Health Sci Rev. 2022;5:100063. https://doi.org/10.1016/j.hsr.2022.100063
7. Stompor-Gorący M, Machaczka M. Recent advances in biological activity, new formulations and prodrugs of ferulic acid. Int J Mol Sci. 2021;22(23):12889. https://doi.org/10.3390/ijms222312889.
8. Kumar N, Pruthi V. Potential applications of ferulic acid from natural sources. Biotechnol Rep (Amst). 2014;4:86–93. https://doi.org/10.1016/j.btre.2014.09.002.
9. Ye L, Hu P, Feng LP, Huang LL, Wang Y, Yan X, Xiong J, Xia HL. Protective effects of ferulic acid on metabolic syndrome: A comprehensive review. Molecules. 2022;28(1):281. https://doi.org/10.3390/molecules28010281.
10. Zhai Y, Wang T, Fu Y, Yu T, Ding Y, Nie H. Ferulic acid: A review of pharmacology, toxicology, and therapeutic effects on pulmonary diseases. Int J Mol Sci. 2023;24(9):8011.: https://doi.org/10.3390/ijms24098011.
11. Liu Y, Shi L, Qiu W, Shi Y. Ferulic acid exhibits anti-inflammatory effects by inducing autophagy and blocking NLRP3 inflammasome activation. Mol Cell Toxicol. 2022;18(4):509–519. https://doi.org/10.1007/s13273-021-00219-5.
12. Adeyi E, Oluwatobi S, Ajayi B, Adewale J, Taiwo A, Daniel O, Ebunoluwa O, Ebenezer S, Iyabode M. The anti-inflammatory effect of ferulic acid is via the modulation of NFκB-TNF-α-IL-6 and STAT1-PIAS1 signaling pathways in 2-methoxyethanol-induced testicular inflammation in rats. Phytomedicine Plus. 2023;3:100464. https://doi.org/10.1016/j.phyplu.2023.100464.
13. Mir SM, Ravuri HG, Pradhan RK, Narra S, Kumar JM, Kuncha M, Kanjilal S, Sistla R. Ferulic acid protects lipopolysaccharide-induced acute kidney injury by suppressing inflammatory events and upregulating antioxidant defenses in Balb/c mice. Biomed Pharmacother. 2018;100:304-315. https://doi: 10.1016/j.biopha.2018.01.169.
14. Aarabi A, Honarvar M, Mizani M, Faghihian H, Gerami A. Extraction and purification of ferulic acid as an antioxidant from sugar beet pulp by alkaline hydrolysis. Ital J Food Sci. 2016;28(3):362-375. doi: 10.14674/1120-1770/ijfs.v143.
15. Bajpai VK, Majumder R, Park J. Isolation and purification of plant secondary metabolites using column-chromatographic technique. Bangladesh J Pharmacol. 2016;11(4):844. doi: 10.3329/bjp.v11i4.28185.
16. Kowalska T, Kaczmarski K, Prus W. Theory and mechanism of thin-layer chromatography. In: Sherma J, Fried B, editors. Handbook of Thin-Layer Chromatography. 3rd ed. Revised and Expanded. New York: Marcel Dekker; 2003. p. 47-80.
17. Snyder LR, Kirkland JJ, Glajch JL. Practical HPLC Method Development. 1st ed. New York: John Wiley and Sons; 1997. doi:10.1002/9781118592014.
18. Zhao X, Wang M, Zhang Y, Zhang Y, Tang H, Yue H, Zhang L, Song D. Macrophages in the inflammatory response to endotoxic shock. Immun Inflamm Dis. 2024;12(10):e70027. doi: 10.1002/iid3.70027.
19. Yang Y, Kim SC, Yu T, Yi YS, Rhee MH, Sung GH, Yoo BC, Cho JY. Functional roles of p38 mitogen-activated protein kinase in macrophage-mediated inflammatory responses. Mediators Inflamm. 2014;2014:352371. doi: 10.1155/2014/352371.
20. Kim C, Sano Y, Todorova K, Carlson BA, Arpa L, Celada A, Lawrence T, Otsu K, Brissette JL, Arthur JS, Park JM. The kinase p38 alpha serves cell type-specific inflammatory functions in skin injury and coordinates pro- and anti-inflammatory gene expression. Nat Immunol. 2008;9(9):1019-27. doi: 10.1038/ni.1640.
21. Alves E, Bannimath G, Prabhakaran P, Parameswaran S, Awasthi A. Targeting breast cancer: Unveiling FN3K enzyme inhibitors via structure-based virtual screening and molecular dynamic simulation. IJNRD - International Journal of Novel Research and Development. 2024;9(6). https://ijnrd.org/papers/IJNRD2406239.pdf
22. M A, I MA, Ramalingam K, S R. Evaluation of the Anti-inflammatory, Antimicrobial, Antioxidant, and Cytotoxic Effects of Chitosan Thiocolchicoside-Lauric Acid Nanogel. Cureus. 2023;15(9):e46003. doi: 10.7759/cureus.46003.
23. Mans DRA, Friperson P, Djotaroeno M, Sewberath Misser V, Pawirodihardjo J. *In vitro* anti-inflammatory and antioxidant activities and phytochemical content of the fresh stem juice from *Montrichardia arborescens* Schott (Araceae). Pharmacogn J. 2022;14:296-304. doi: 10.5530/pj.2022.14.99.